

Laser measurements on experiments on plate girders with a very slender web under pure bending

Abspoel, Roland

Publication date

2016

Document Version

Final published version

Published in

ICCCBE2016

Citation (APA)

Abspoel, R. (2016). Laser measurements on experiments on plate girders with a very slender web under pure bending. In N. Yabuki, & K. Makanae (Eds.), *ICCCBE2016: Proceedings of the 16th International Conference on Computing in Civil and Building Engineering, Osaka, Japan* (pp. 1-8). ICCCB2016 Organizing Committee.

Important note

To cite this publication, please use the final published version (if applicable). Please check the document version above.

Copyright

Other than for strictly personal use, it is not permitted to download, forward or distribute the text or part of it, without the consent of the author(s) and/or copyright holder(s), unless the work is under an open content license such as Creative Commons.

Takedown policy

Please contact us and provide details if you believe this document breaches copyrights. We will remove access to the work immediately and investigate your claim.

Laser measurements on experiments on plate girders with a very slender web under pure bending

Roland Abspoel¹

1) Ph.D., Principal Research Scientist, Delft University of Technology, Delft, The Netherlands. Email: r.abspoel@tudelft.nl

Abstract:

This paper is about the laser measurements as part of the research on the distribution of a certain amount of steel over the flanges and the web of an I-shaped plate girder to achieve the maximum bending moment resistance [1]. In many steel structures standard hot-rolled sections are used. These sections are divided into specific types in Europe and similar profiles in the USA. The range of hot-rolled sections is limited and therefore fabricated plate girders are used.

Double symmetric I-shaped plate girders are built up with steel plates for the top and bottom flange and the web, welded together to a cross-section. Using this type of plate girders, a high degree of optimisation of material use is possible by using different plate thicknesses and widths for the flanges and thickness and height for the web. In the thesis the main topic for optimisation is the bending moment resistance of a plate girder.

The maximum bending moment resistance appears for plate girders with a lot of material in the flanges and with a large web height. The web thickness has to be as small as possible and so the web slenderness has to be as large as possible. The limitation of the web slenderness is according to the Eurocode and the American standard based on flange induced buckling. The web of cross-section class 4 buckles and this buckling is during experiments measured by lasers.

This paper gives an overview of the results of the laser measurements. Based on these measurements, it is concluded that flange induced buckling is not a limitation for the web slenderness. High web slenderness can be applied and the bending moment resistance increases enormously and the stiffness increases even more. Because of this, the use of HSS becomes of high interest.

Keywords: plate girders, web slenderness, lasers measurements.

1. INTRODUCTION

In many steel structures like buildings, industrial halls and bridges, standardised hot-rolled sections are used. The range of hot-rolled sections is limited and therefore fabricated plate girders are used when these standardised hot-rolled sections do not meet the requirements for stiffness, strength, stability and economy.

Such a plate girder is built up from steel plates for the top and bottom flange and for the web, welded together to an I-shape cross-section, single or double symmetric. Using this type of plate girders, a high degree of optimisation of material use is achieved by using different plate thickness and width for the flanges, and thickness and height for the web over the span of the girder, adapted to the distribution of bending moments and the shear forces.

Optimisation can be carried out for many aspects, but in the thesis the ultimate bending moment resistance of a plate girder, given a certain weight per unit length, is the main topic for optimisation. In many cases, when using hot-rolled sections, the stiffness is the decisive design criterion and therefore using high strength steel grades seems not useful. For plate girders with the same cross-sectional area as a hot-rolled section, the stiffness is much higher and the strength of the material can be better exploited, so using higher steel grades can be useful.

In case of a fixed cross-sectional area, by increasing the lever arm, more material is placed in the web, reducing the remaining material for the flanges. However, the lever arm can also be increased without using more material in the web by increasing the web height and decreasing the web thickness. This process is restricted by a limit for a practical thickness of the web, to enable welding of the section and also the handling of the plate girder.

The web slenderness, expressed in the height to thickness ratio of the web plate, needs not be restricted. Reaching the elastic critical plate buckling stress in the web is hardly of influence on the bending moment resistance of the plate girder, see Abspoel [1] and [2]. The post-critical plate buckling behaviour of the web plate can be easily exploited using the effective width theory.

However, EN1993-1-5 [4] and the AISC 360-10 [6] limit the web slenderness by a specific phenomenon called “flange induced buckling”. This phenomenon has been studied by Basler [3] and is described as “vertical buckling of the compressive flange into the web”. Basler based this maximum web slenderness only on one laboratory test results and so it was considered of interest to perform additional research on this limitation to investigate whether this phenomenon really limits the bending moment resistance of a plate girder and see if it is

possible to increase this maximum web slenderness.

At the Stevin II Laboratory of the Delft University of Technology 10 model-scale plate girders are subjected to a four point bending test, similar to the test specimen G4 of Basler, see Abspoel [1]. The initial lateral imperfections of the web are measured by using lasers. After every deformation driven step the tests are stopped to measure the development of these initial imperfections.

2. DELFT EXPERIMENTS

The maximum web slenderness according to EN1993-1-5 [4] is limited to:

$$\beta_{w,max} = 0.55 \cdot \frac{E}{f_{y,tf}} \cdot \sqrt{\frac{A_w}{A_f}} \quad (1)$$

where E : Young's modulus,
 $f_{y,tf}$: yield stress of the top flange,
 A_w : web area
 A_f : area of the top flange

The nominal web dimensions are: web thickness $t_w = 1$ mm and the web height h_w varies 400 mm, 600 mm and 800 mm. The nominal dimensions for the flanges $b \times t_f$ are 50×4 mm², 80×5 mm² and 100×4 mm². The actual dimensions, the web slenderness based on these dimensions and the maximum web slenderness based on the actual dimensions of the test girders and the actual steel grade of the compressive flanges are shown in Table 1.

Table 1. Dimensions of the Delft Experiments

| | h_w [mm] | t_w [mm] | b [mm] | t_f [mm] | β_w [-] | $\beta_{w,max}$ [-] | ρ [-] |
|--------------|---------------|---------------|-------------|---------------|------------------|------------------------|---------------|
| 1, 400x50 | 400.0 | 1.01 | 49.7 | 4.36 | 396.1 | 471.2 | 1.87 |
| 2, 400x80(1) | 399.3 | 1.00 | 80.0 | 5.40 | 399.3 | 344.7 | 0.92 |
| 3, 400x80(2) | 399.8 | 1.02 | 80.1 | 5.57 | 392.0 | 349.6 | 0.91 |
| 4, 400x100 | 400.1 | 0.93 | 98.7 | 4.29 | 430.2 | 315.7 | 0.88 |
| 5, 600x50 | 601.6 | 1.02 | 49.6 | 4.48 | 589.8 | 585.0 | 2.76 |
| 6, 600x80 | 600.2 | 0.97 | 79.9 | 5.53 | 618.7 | 403.1 | 1.32 |
| 7, 600x100 | 600.1 | 0.97 | 99.1 | 4.31 | 618.7 | 395.5 | 1.36 |
| 8, 800x50 | 801.0 | 0.97 | 50.2 | 4.40 | 825.8 | 664.2 | 3.51 |
| 9, 800x80 | 799.4 | 0.98 | 80.2 | 5.60 | 815.7 | 476.8 | 1.75 |
| 10, 800x100 | 799.4 | 1.00 | 98.8 | 4.24 | 799.4 | 470.7 | 1.91 |

Table 1 shows that the web slenderness β_w of eight of ten test girders is smaller than the maximum web slenderness $\beta_{w,max}$ and so it is expected that the girders will fail by flange induced buckling. The maximum web slenderness of test girder 1, 400x50, (nominal web height is 400 mm and the flange width is 50 mm) is larger than the actual web slenderness. For test girder 5, 600x50, is the web slenderness close to the maximum web slenderness. Several instruments are used during testing to measure loads, deformations and strains, see Figure 1.

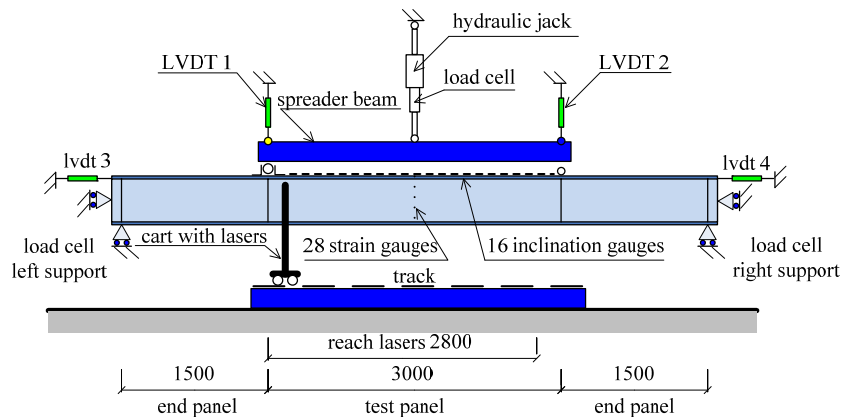


Figure 1. Test rig including a test girder and the instrumentation

A specific cart is designed including horizontal and vertical lasers, see Figure 2. The horizontal lasers are used to measure the out-of-plane deformations of the web of the test panel and the vertical deflections of the tips of the top flange. The vertical lasers are used to measure the vertical deformation of the test girders, but also to measure the rotation of the bottom flange. During driving of the cart over the track, the vertical position of the horizontal lasers is adapted to the vertical deflection of the test specimen by the measurements of the vertical laser in the centre of the bottom flange, to make sure that the horizontal deflections of the web are measured every time at the same material points of the web. The longitudinal position of the cart is measured with a steel rope, see Figure 3.

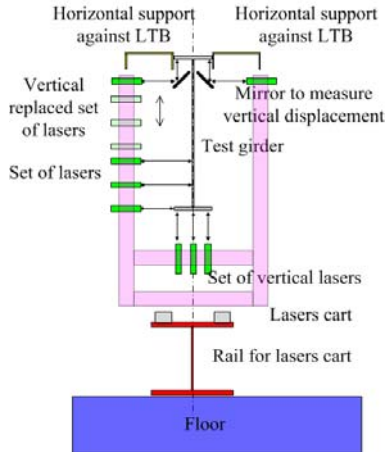


Figure 2. Cart with lasers

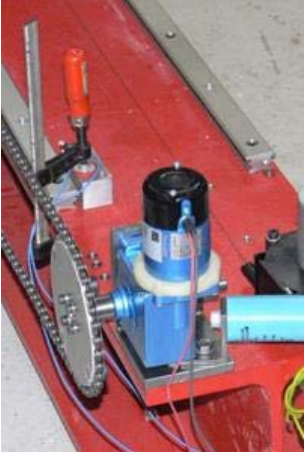


Figure 3. Motor for the cart and Lvdt with steel rope

3. RESULTS

The horizontal lasers measured the total out-of-plane deformations of the web in the test panel after every deformation step. The initial deformation step is step 0 and next steps are starting from A up to, for example AG, depending on the number of deformation steps. The out-of-plane deformations are presented in graphs. Based on these total out-of-plane deformations, additional graphs are made, namely the out-of-plane deformations as function of the load, so the total deformations minus the initial deformations, and the increment of the out-of-plane deformations, so the total deformations of step *i* minus the total deformations of the step *i*-1. Due to the limited number of pages of this paper, the results of two test girders will be shown in this paper, namely of test girder 4, 400x100, and 8, 800x50. Figures 4, 5 and 6 show the total out-of-plane deformations of test girder 4, 400x100, for deformation step 0, M for which the maximum actuator force appeared and N. The figure which shows the last deformation step shows the legends for all previous deformation steps too. It can be seen that the amplitudes changed up to deformation step M. After deformation step N the number of buckles changed, the amplitudes increased and at the right-hand side of the test panel in the area 161-201 a snap through occurred.

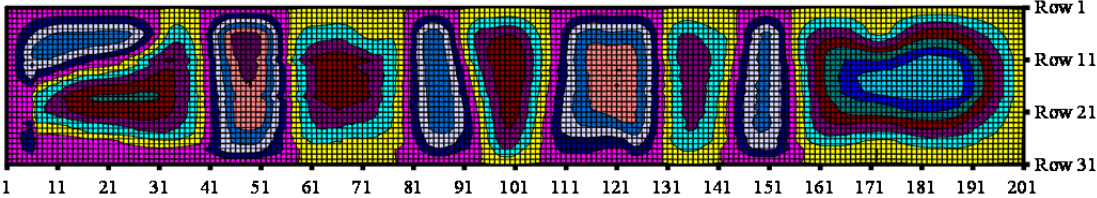


Figure 4. The total out-of-plane deformations, step 0, girder 4, 400x100

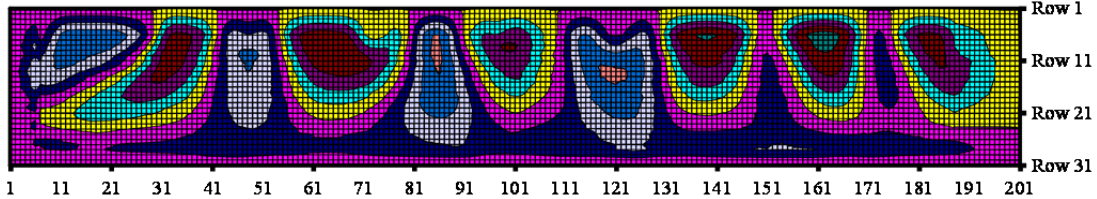


Figure 5. The total out-of-plane deformations, step M, girder 400x100

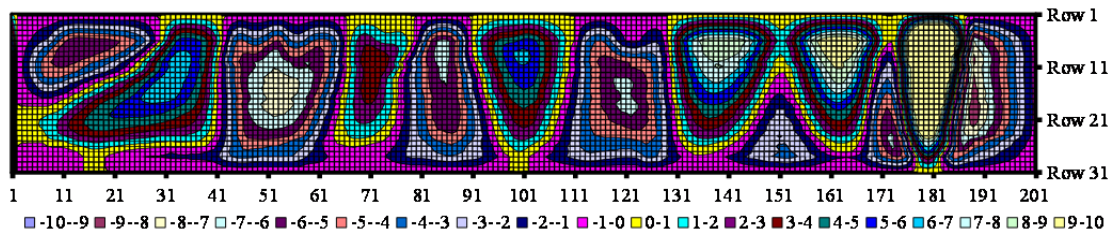


Figure 6. The total out-of-plane deformations, step N, girder 400x100

For test girder 8, 800x50 the initial out-of-plane deformations are shown in Figure 7 and for step J for which the maximum actuator force appeared and step K and O in Figures 8 to 10. The girder failed at the left side.

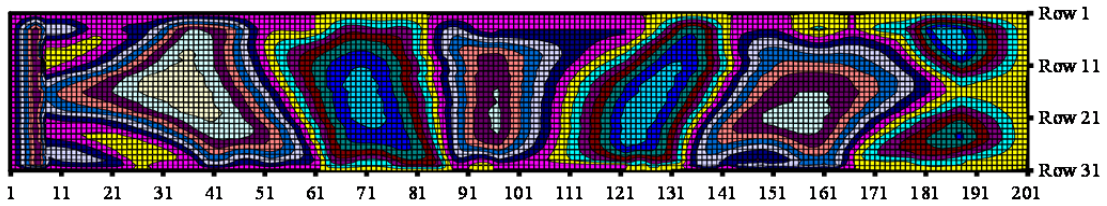


Figure 7. The total out-of-plane deformations, step 0, girder 8, 800x50

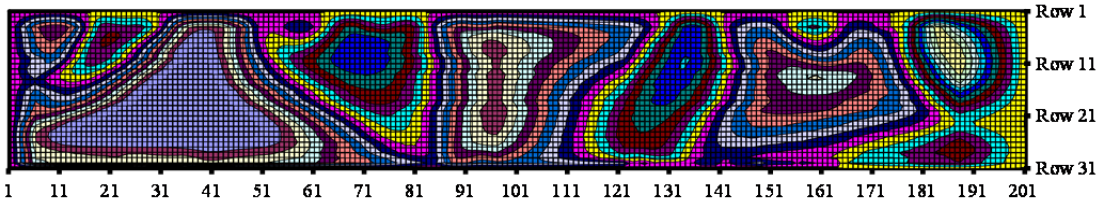


Figure 8. The total out-of-plane deformations, step J, girder 8, 800x50

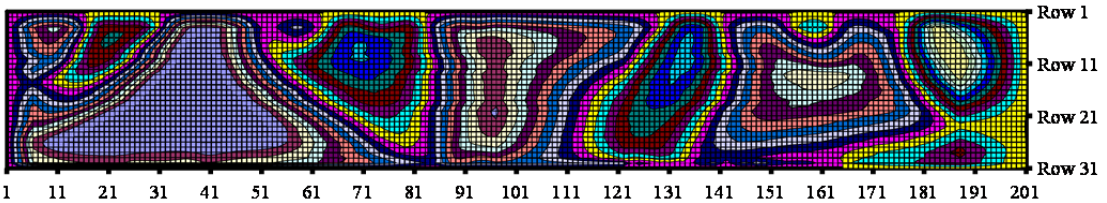


Figure 9. The total out-of-plane deformations, step K, girder 8, 800x50

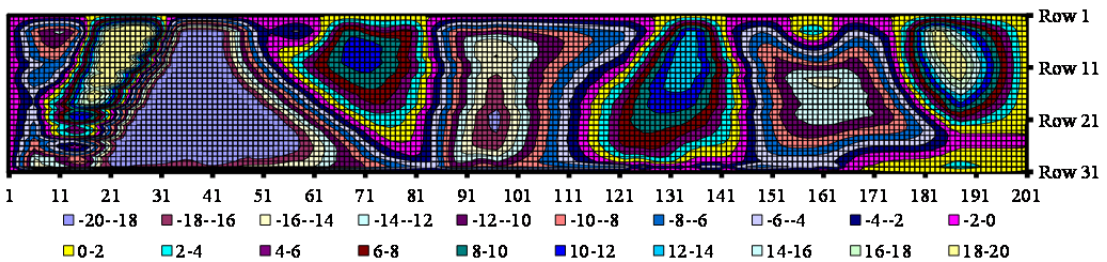


Figure 10. The total out-of-plane deformations, step O, girder 8, 800x50

This test girder 8, 800x50, behaved different from the test girder 4, 400x100. At the moment the maximum actuator force occurred in deformation step J, see Fig. 8, the amplitude of one of the buckles at the left increased strongly compared with the initial unloaded situation, see Fig. 7. In the next deformation step K, see Fig. 9, there is no flange induced buckling. This flange induced buckling occurred in deformation step O, after an enormously increase of the amplitude in a rather small buckle close at the left-hand load introduction.

It is of interest to look at the changes of the out-of-plane deformations after starting the test, the out-of-plane deformations as function of the load and the increment out-of-plane deformations. Figs. 11 and 12 show for test girder 4, 400x100, that the out-of-plane deformations of step M and N respectively, are the largest at the right-hand part of the test panel, close to the load introduction. Figs. 13, 14 and 15 show for test girder 8, 800x50,

that the out-of-plane deformations of step J, K and O respectively, are the largest at the left-hand part of the test panel, close to the left-hand load introduction.

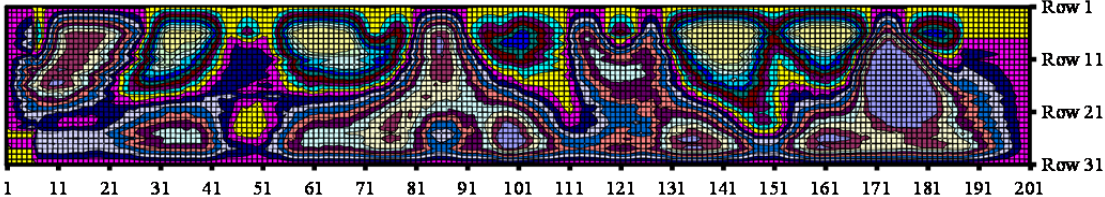


Figure 11. The out-of-plane deformations as function of the load, step M, girder 4, 400x100

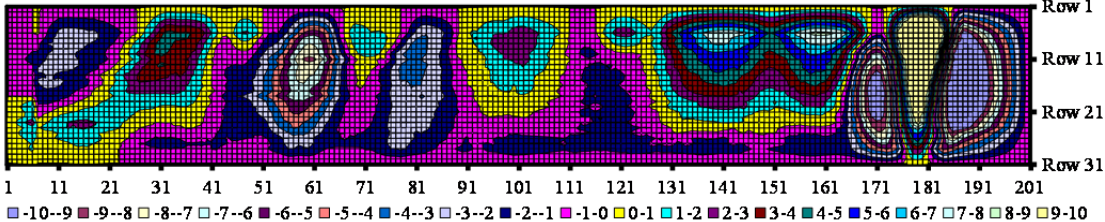


Figure 12. The out-of-plane deformations as function of the load, step N, girder 4, 400x100

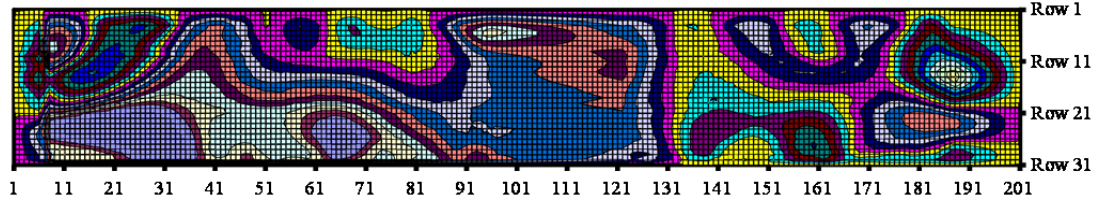


Figure 13. The out-of-plane deformations as function of the load, step J, girder 8, 800x50

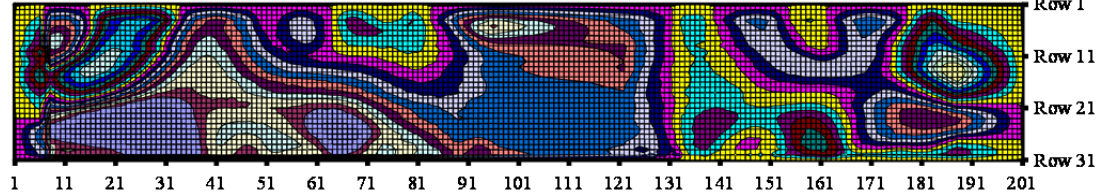


Figure 14. The out-of-plane deformations as function of the load, step K, girder 8, 800x50

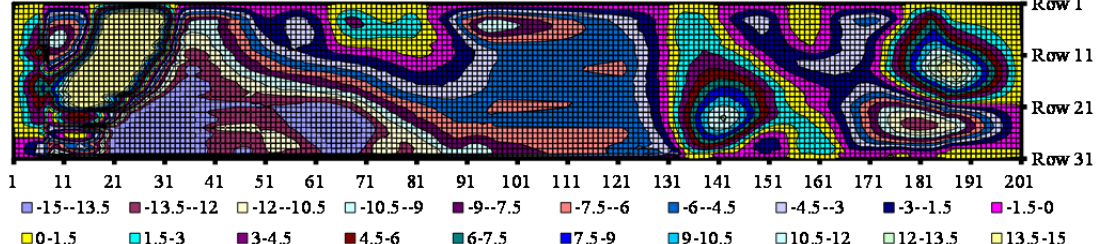


Figure 15. The out-of-plane deformations as function of the load, step O, girder 8, 800x50

Next to these out-of-plane deformations as function of the loading, the increment out-of-plane deformations can be presented. Figs. 16 and 17 show the increment out-of-plane deformations for test girder 4, 400x100, for step M and N. It is clear that in deformation step M the incremental out-of-plane deformations are rather small, more or less uniformly distributed over the span of the test panel according to the pattern of the buckles. In deformation step N the incremental out-of-plane deformations increases suddenly and as seen in the other graphs, the most at the right-hand part of the web in the test panel.

For test girder 8, 800x50, the incremental out-of-plane deformations show the same location for the final failure

as the total out-of-plane deformations and the out-of-plane deformations as function of the loading. The largest deformations appears at the left-hand part of the test panel.

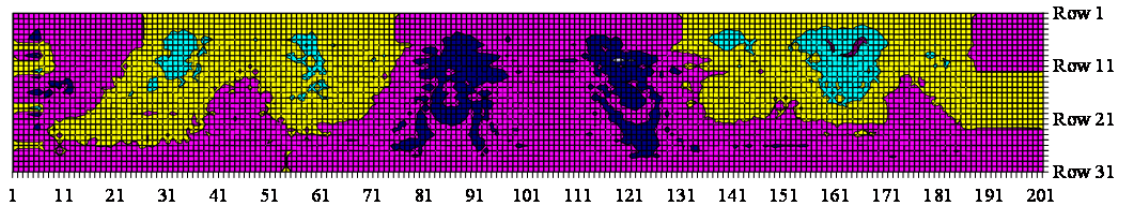


Figure 15. Increment out-of-plane deformations, step M, girder 4, 400x100

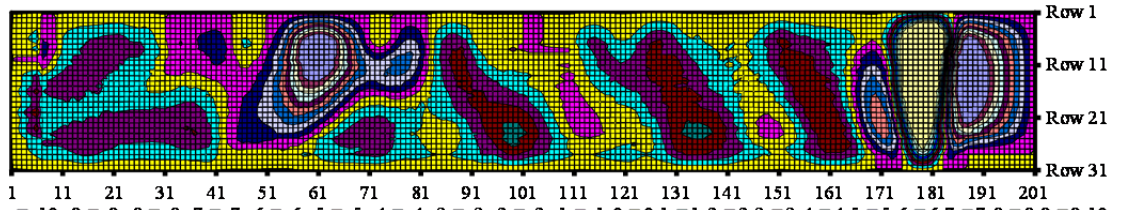


Figure 16. Incremental out-of-plane deformations, step N, girder 4, 400x100

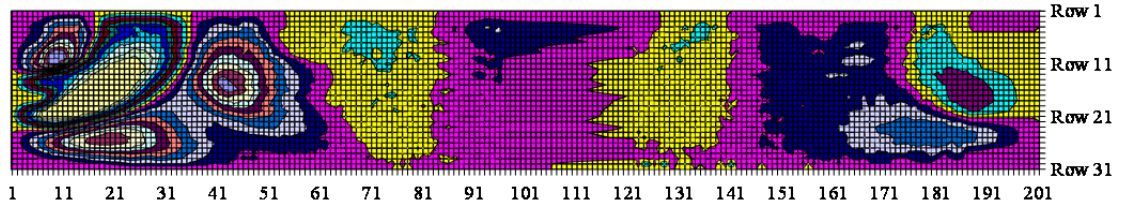


Figure 17. Incremental out-of-plane deformations, step J, girder 8, 800x50

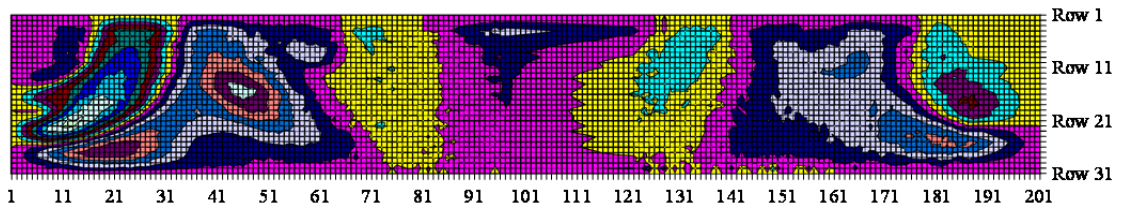


Figure 18. Incremental out-of-plane deformations, step K, girder 8, 800x50

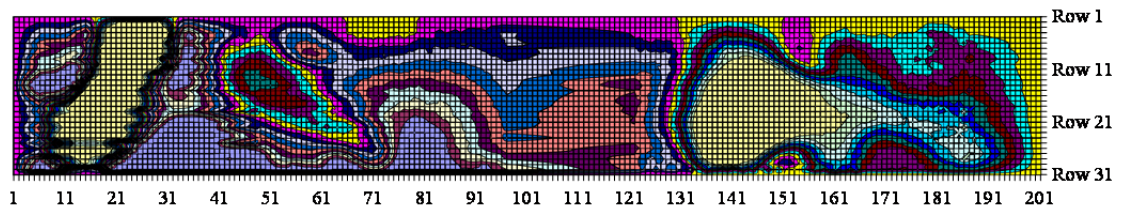


Figure 19. Incremental out-of-plane deformations, step O, girder 8, 800x50

The buckle patterns of the web in the test panel show rather accurately the location where flange induced buckling occurred in the compressive flange.

Next to the out-of-plane deformations of the web in the test panel, the vertical deflections of the tips of the top flange are measured by lasers by using mirrors under 45°. The difference in vertical deflections, see Fig. 19, can be used to determine the rotation of both flanges. Fig. 19 shows that the difference in vertical deflections increases at the right-hand side of the test panel. In the deformation step N the measurements become inaccurate and gives a fully different view of the graph, it looks like the mirror was hit by the web. The vertical deflections of the tips of the bottom flange and the centre of the bottom flange are directly measures by vertical lasers.

During testing the fourth test girder in sequence, girder 1, 400x50, the mirrors broke because of the huge increase of the buckles. The vertical deflections of the top flange are not measured by the lasers for test girders

with a web slenderness of 600 and 800 and the rotations are directly measured by inclination gauges. This is not part of this paper. Flange induced buckling is always introduced by a large increase in rotation, see Fig. 19.

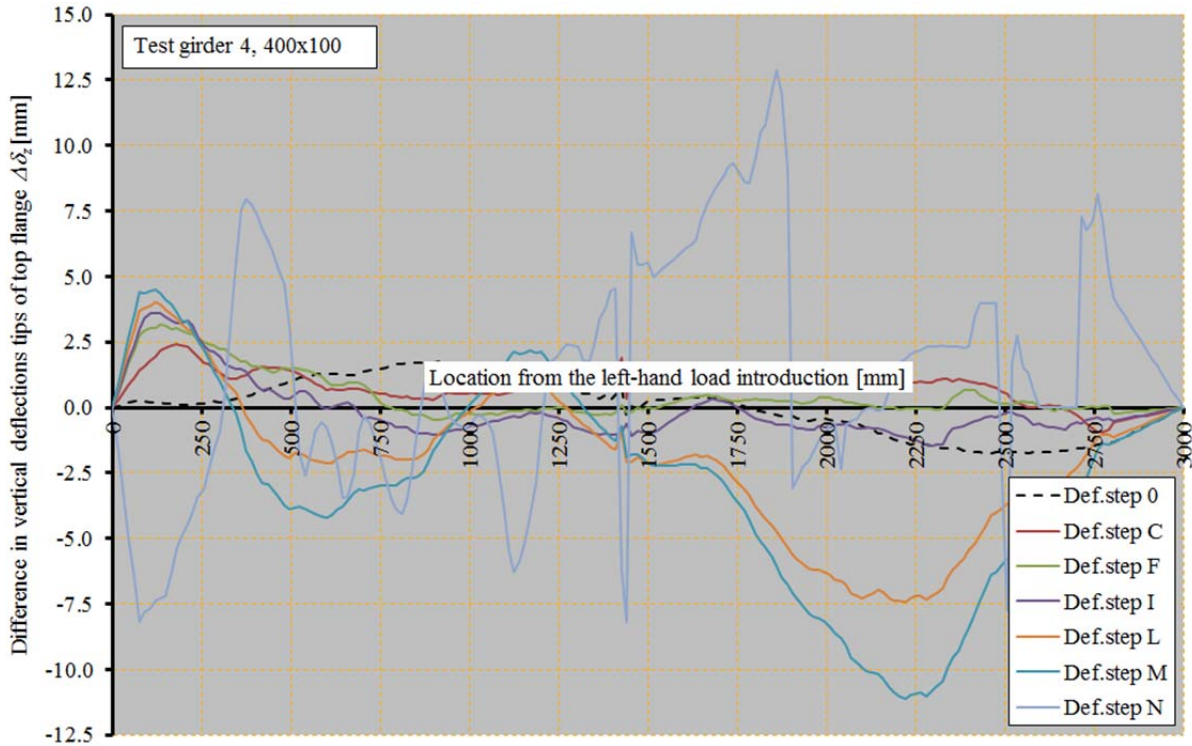


Figure 19. Difference in deflections of the tips of the top flange [mm], girder 4, 400x100

Next to this, the vertical deformation in the middle of the bottom flange is measured. Figs. 20 and 21 present the vertical deflections of the bottom flange for test girder 4, 400x100, and girder 8, 800x50, respectively. The location of the flange induced buckling is clearly shown in the figures.

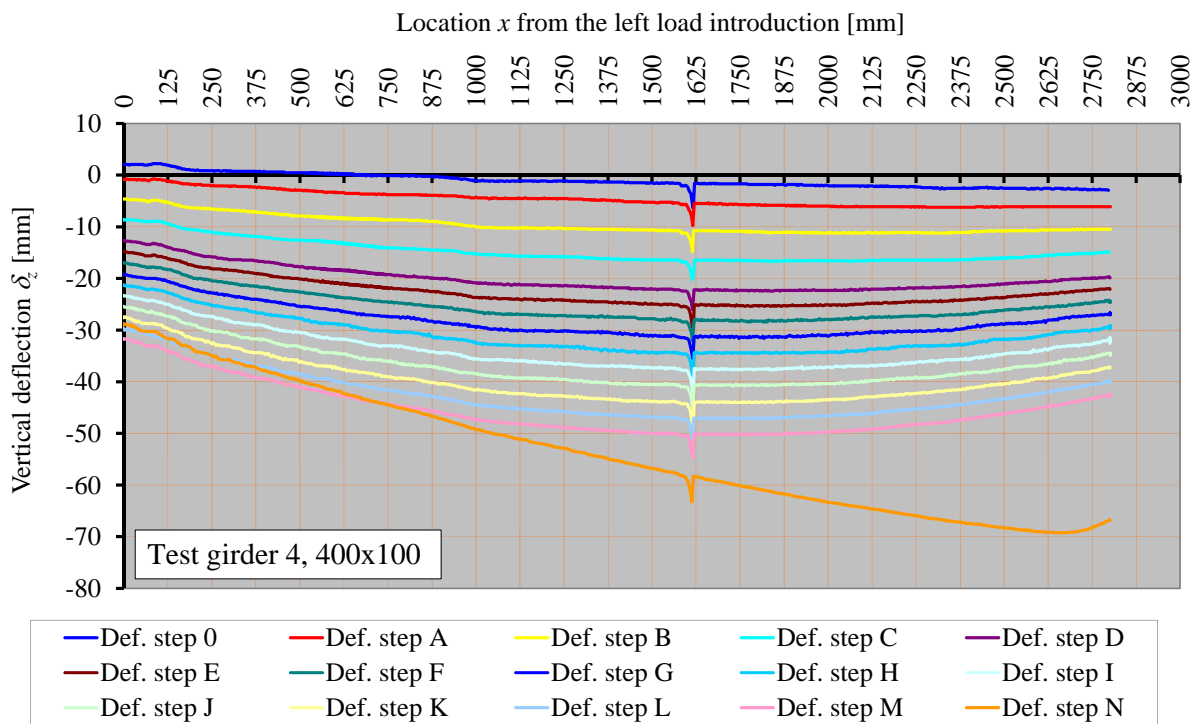


Figure 20. Vertical deflections of the bottom flanges measured by laser, girder 4, 400x100

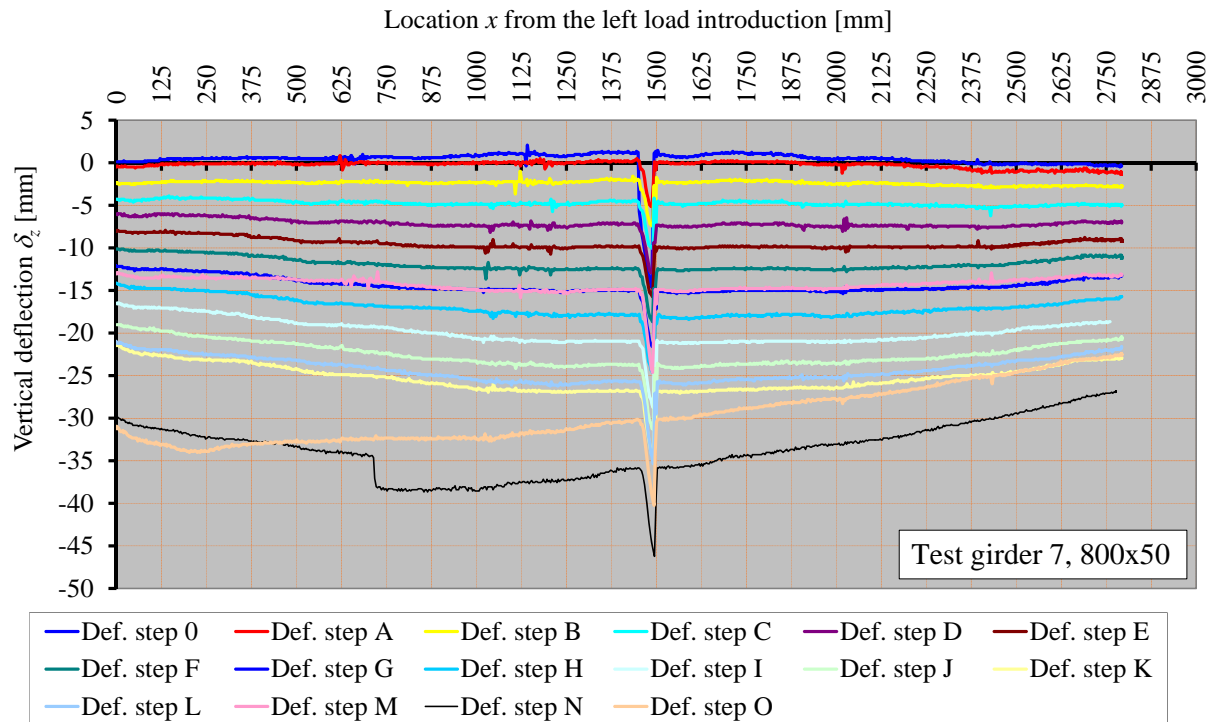


Figure 21. Vertical deflections of the bottom flanges measured by laser, girder 8, 800x50

From the results of two of ten test girders of the Delft experiments it is shown in this paper that the bending moment resistance is not determined by flange induced buckling as adopted in EN1993-1-5 as well as in AISC 360-10. Abspoel [1] and [2] proved this for the other test girders too.

5. CONCLUSIONS

The following conclusions are drawn focussed on measurements with lasers on plate girders with a very slender web after every deformation step:

- The total out-of-plane deformations can be used to show the location of the final failure mechanism, flange induced buckling, which appears after the maximum load occurred;
- Next to the total out-of-plane deformations the deformations as function of the loading and the increment out-of-plane deformations can be determined which indicates the same location of the final failure mechanism, sometimes even more clear;
- The vertical deflections at the tips of the top flange can be useful to measure the rotation of the compressive flange, but the use of mirrors is very sensitive to break by the large out-of-plane deformations of the very slender web;
- The vertical deflections in the centre of the bottom flange is useful to show the location of the final failure, flange induced buckling over the span of the test girder.

REFERENCES

- [1] Abspoel R. "Optimisation of plate girders", *Dissertation*, Delft University, The Netherlands, 2015.
- [2] Abspoel R. "Plate girders under bending", *Conference paper*, SDDS2015, Romania, 2016
- [3] Basler K. "Strength of plate girders", *Dissertation*, Lehigh University, Bethlehem, USA, 1959.
- [4] EN1993-1-5, Eurocode 3: Design of steel structures – Part 1-5 Plated structural elements, 2006
- [5] EUR8849, Draft Eurocode 3: Common unified rules for steel structures, 1984
- [6] AISC 360-10, Specification for structural steel buildings, American Institute of Steel Constructions, 2010